Kütahya Dumlupınar University
Institute of Graduate Studies

Journal of Scientific
Reports-A
E-ISSN: 2687-6167
Number 52, March 2023

RESEARCH ARTICLE

285 nm AlGaN-BASED DEEP-ULTRAVIOLET LED WITH HIGH INTERNAL QUANTUM EFFICIENCY: COMPUTATIONAL DESIGN

İrem ÖNER ALP[1*], Bilgehan Barış ÖNER[2], Esra EROĞLU[3]

[1*]Gazi University, Faculty of Sciences, Department of Physics, Ankara, iremoner@gazi.edu.tr, ORCID: 0000-0002-6937-7864
[2]Gazi University, Faculty of Sciences, Department of Physics, Ankara, baris.oner@roketsan.com.tr,
ORCID: 0000-0001-9440-2235
[3]METU, Faculty of Engineering, Department of Mechanical Engineering, Ankara, esraer@metu.edu.tr,
ORCID: 0000-0002-6848-5142

Receive Date:26.10.2022 *Accepted Date: 22.01.2023*

ABSTRACT

In this paper, the systematic computational design process of AlGaN-based multiple quantum-well (QW) deep-ultraviolet (DUV) light-emitting diode (LED) grown on sapphire (Al_2O_3) substrate was investigated. An optimization was held to increase internal quantum efficiency (IQE) handling the LED parameters such as doping percentage of the n- and the p-type layers of these devices. The structure parameters of the best design were determined through a customized genetic algorithm integrated into the nanostructure quantum electronic simulation (nextnano). As a determining factor, IQE was obtained to be 24% for the devised 285 nm LED. It has been demonstrated that this result can be increased up to a remarkably high value of 70% by a low threading dislocation density (TDD) and reduced Auger recombination. In addition, the operation input power and potential difference were successfully kept below 0.1 W/mm^2 and 5.05 V, respectively.

Keywords: *Deep-ultraviolet LED, UV-C LED, Quantum efficiency, Genetic algorithm*

1. INTRODUCTION

It is predicted that the biomedical application area of deep-ultraviolet (DUV) light-emitting diode (LED) systems will become widespread during and after the pandemic period [1-3]. However, the efficiencies of the devices with DUV radiation (20%) [4] have not yet reached the desired levels and are still a topic of current research. Deactivation of microorganisms such as viruses and bacteria is provided by irradiation in the UV-C range of 250 to 280 nm depending on their biological structures [5, 6]. Although the region where deactivation is most effective is below 265 nm, LED devices operating up to 300 nm can be preferred in order not to damage human cells [7]. Otherwise, UV-C LEDs have been extensively utilized in chemical detection through the fluorescence characteristics of some materials induced by UV-C light [8] and in drinking water decontamination due to the remarkable results achieved [9-12]. In this context, the selection criteria for the materials suitably

JSR A
Journal of Scientific Reports

qualified depend on factors such as efficiency percentage, manufacturability, easy availability, and environmental friendliness (non-toxicity).

The AlGaN alloy emits photons in the UV-C region, which can be controlled by adjusting the Al/Ga ratio and the other optoelectronic parameters. In addition, Al/In doped III-V compounds also play an important role in the determination of the operating wavelength and efficiency [13, 14]. At this point, the active region thickness and the concentrations in compounds predicted for a LED design are of crucial significance. For example, the higher the Al amount, the more dislocations appear in practice yielding adverse effects on the required optical properties [15]. Besides, low mismatch percent for the layers is important in crystal growth and the AlGaN-based LED structure with the AlN buffer layer examined in this paper can be grown on sapphire (Al_2O_3) as it is often reported in the literature [16-20]. The various difficulties encountered during the production process apart from the ones mentioned, such as point defects, cracking issues, low hole concentration, junction heating effect, and low light extraction efficiency (LEE) should not be ignored as well [7]. Thus, high device efficiency will be obtained along with overcoming these handicaps.

Multiple research groups have carried out extensive examinations on DUV LED design and features of the constituent materials for several years yielding significant progress in performance [8, 21-27]. One of the most recent studies performed by Hirayama et al. have introduced an AlGaN UV-C LED with high power in which a photonic crystal reflector was used [28]. Jain et al. proposed graded staircase quantum barriers against electron leakage problem for AlGaN DUV LEDs [29]. A high LEE was measured by Zhang et al. for Ag-nanodots and Al electrodes adoption on AlGaN LED operating at ~280 nm [30]. Itokazu et al. were previously able to establish an improvement in AlGaN DUV LED performance via high-temperature annealing with an additional growth process for the AlN layer [31]. Shin et al. managed to get an enhanced LEE in a ~267 nm AlGaN nanowire LED with photonic crystal [32]. Average package power values were obtained over 0.1 mW for AlGaN UV-C LEDs emitting in the range of 230-240 nm by Moe et al. and the optical and electrical properties were characterized [33]. Chen et al. theoretically aimed to increase LEE choosing the contact layer as graphene in the deep UV LED block without p-GaN and have had a notable result [34].

The internal quantum efficiency (IQE), the enhancement of which is the subject of this study, is the other key factor that affects the LED efficiency and there have been significant attempts from researchers to improve IQE [35-39]. Shim et al. have proposed a method of temperature-independent measurement for IQE [40]. It is predicted that a very high-valued IQE for 284 nm InAlGaN UV-C LED and have grown the DUV LEDs onto Al on sapphire operating at 222-282 nm [41]. By defect engineering, a similar result was obtained for IQE of 280 nm LED [42]. Hao et al. determined 267 nm LED IQE through a fitting method to electroluminescence data [43] and an increment on IQE value for AlGaN-based DUV LED was observed by the use of nano patterned sapphire substrates yielding low dislocation density [44]. Guttmann et al. have studied IQE of AlGaN LEDs operating at 263 nm that has p-AlGaN layers with different separate Al mole fractions [45].

In this paper, we have presented a systematic computational optimization process of DUV light-emitting devices to increase inner efficiency while minimizing the input power. IQE improvement of multi-layered quantum-well (QW) region including AlGaN with AlN interlayer (IL) was addressed in

an algorithm which was developed by authors for the current study. The electron blocking layer (EBL) has been used because of the remarkable direct transition energy range in UV. In the next Section, the optimization method has been given. This step on IQE was performed by nanostructure quantum electronic simulation. Afterward, achieved results are reported for the LED structure with low-mismatch design and a discussion with the current literature is given. Finally, concluding remarks are written as a short summary.

2. MATERIAL AND METHOD

An ultraviolet multi-quantum well LED emitting under 300 nm wavelength has been aimed to design in this part of the study. An optoelectronic semiconductor nanodevice software package of nextnano was used [46, 47]. AlGaN based LED devices have less lattice-mismatch issues due to the compatible lattice constants (a_{AlN} = 4.38 Å, a_{GaN} = 4.50 Å). Therefore, they constitute the basis of the device due to its above-mentioned superiorities over alternative UV materials. The main p-i-n layers of the LED are determined to be: an n-doped junction layer, 5 QW layers, a p-doped electron blocking layer (EBL) and finally a p-doped junction layer. QWs consist of a thinner $Al_xGa_{(1-x)}N$, a thicker $Al_yGa_{(1-y)}N$ and an AlN interlayer (IL) between each quantum well. This brings 5 thickness, 3 doping and 6 alloy concentration degrees of freedom and therefore a total of 15 design parameters including input potential difference between p and n layers V_{pn}. These parameters are possible to be arranged such that a relatively high internal quantum efficiency value can be achieved for a low input power P_{in} for peak luminosity (λ_{PL}) wavelength under 300 nm. In order to construct such a design, here we utilize a conventional genetic algorithm as the optimization method which was written and developed by authors particularly for the current study. The main steps in the algorithm's cycle are given in Figure 1.

JSR A
Journal of Scientific Reports

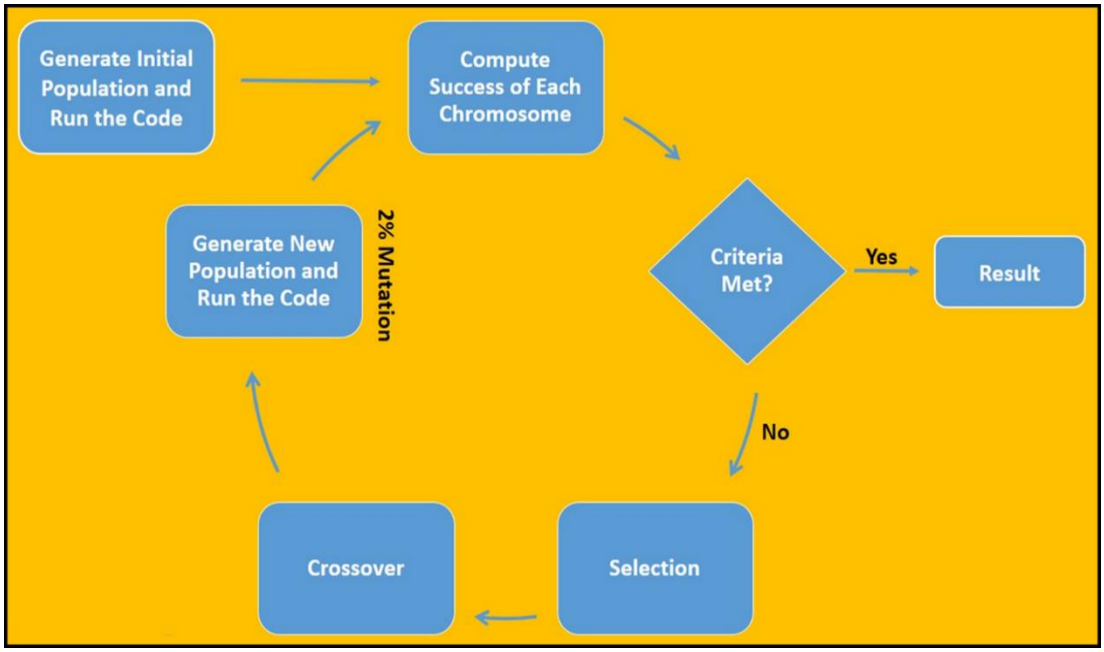

Figure 1. Flow chart of the utilized algorithm to generate highly efficient ultraviolet LED.

The number of chromosomes in each population was chosen as 75. Design parameters played the role of genes and V_{pn} was fixed at 5.00 V during the algorithm cycle. The first population was generated by a random selection (see the second column of Table 1). Success criteria of a chromosome are given by

$$s = \begin{cases} IQE\ , P_{in} < 10\frac{W}{mm^2}\ \lambda_{PL} < 300nm \\ 0, o.w. \end{cases} \quad (1)$$

Chromosomes were sorted after each computation considering their corresponding success rates and they were selected for the next crossover step such that each chromosome was coupled by the subsequent successful chromosome. Couplings began from the worst couples to the best ones. A final coupling was performed between the best and worst chromosomes. Therefore, the number of chromosomes in each population has been fixed. A new chromosome was generated at each crossover step with a 50% chance of getting genes from more and less successful chromosomes and a mutation chance of 2% was given at each turn.

3. RESULTS AND DISCUSSION

We share the results of the optimization via a customized genetic algorithm in Fig. 2 by a normalized success rate. The crossover phase given in the previous section keeps the average success rate low

while enabling a quick rise on each generation. By this means, the desired result (IQE value satisfying the success criteria) has been achieved within the seventh generation. The parameters related to the optoelectronic device design are listed in Table 1 and the third column shows the best results of the genetic algorithm optimization process. The reasonable initial ranges determined from the literature are also given in the second column.

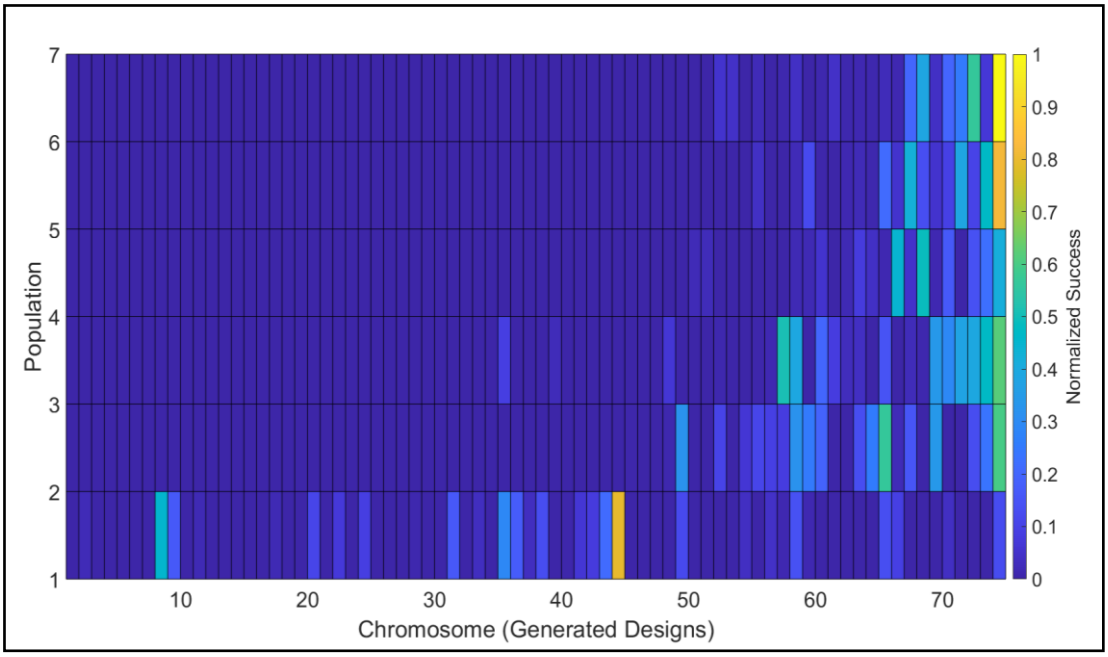

Figure 2. Normalized success rates of each chromosome.

The most effective decrease on the efficiency is due to radiative and nonradiative recombinations rates belonging to Auger and Shockley–Read–Hall (SRH) recombination modes. These phenomena are already known and there are several accepted recombination parameters within DUV region [43, 48]. There are no certain values, computations or direct experimental results standardized for the Auger recombination rate in AlGaN alloys. Therefore, nonradiative-Auger and radiative recombination coefficients were determined to be 2.30×10^{-30} cm^6 s^{-1} and 5.00×10^{-11} cm^3 s^{-1}, respectively [36, 49] and

Table 1. Design parameters of the optoelectronic device, initial population value windows of initial random generation and structure parameters of the best design.

Design Parameter	Parameter Window (if valid)	Best Design
Width of the n-doped layer	100 - 1000 nm	850 nm

JSR A
Journal of Scientific Reports

Width of the QW 1st layer	10 - 15 nm	14.45 nm
Width of the QW 2nd layer	1 - 6 nm	2.66 nm
Width of the IL	0 - 2 nm	1.57 nm
Width of the EBL	15 - 60 nm	57.42 nm
Width of the p-doped layer	30 - 100 nm	95.47 nm
Al% of the n-doped layer	40% - 80%	66%
Al% of the QW 1st layer	40% - 80%	66%
Al% of the QW 2nd layer	30% - 70%	45%
Al% of the EBL	50% - 90%	50%
Al% of the p-doped layer	0 - 2.20e20 cm^{-3}	0
N_d of the n-doped layer	1.00e17 - 2.20e20 cm^{-3}	4.29e19 cm^{-3}
N_d of the QW 2nd layer	5.00e17 cm^{-3}	5.00e17 cm^{-3}
N_a of the EBL	1.00e17 - 2.20e20 cm^{-3}	6.39e17 cm^{-3}
N_a of the p-doped layer	1.00e17 - 2.20e20 cm^{-3}	1.13e19 cm^{-3}
V_{pn}	5.00 V	5.00 V
c_{Auger}	2.30e-30 cm^6s^{-1}	2.30e-30 cm^6s^{-1}
c_{recomb}	5.00e-11 cm^3s^{-1}	5.00e-11 cm^3s^{-1}
τ_n	1.00 e-9 s^{-3}	1.00 e-9 s^{-3}
τ_p	1.00 e-9 s^{-3}	1.00 e-9 s^{-3}
Size	1.00 mm × 1.00 mm	1.00 mm × 1.00 mm

τ_n and τ_p denote radiative lifetimes of free excitons. Another parameter important in the optimization process belongs to the electronic properties. Operating voltage difference between p-contact and n-

JSR A
Journal of Scientific Reports

contact (V_{pn}) was kept fixed at 5.00 V at first since IQE saturates after a certain amount of V_{pn} increment.

The best design has an IQE of 24% when the forward voltage is 5.00 V. In this case, a 1.00 mm × 1.00 mm LED requires an input power below 0.1 W and the LED structure formed according to Table 1 is demonstrated in Fig. 3. From hence, the block is going to be grown on a sapphire substrate and the active region consists of four sequential quantum-well (QW) regions. Each QW includes triple-layers, which are $Al_{0.66}Ga_{0.34}N$ (QW 1st), $Al_{0.45}Ga_{0.55}N$ (QW 2nd) and AlN (IL) from bottom to top with the widths of 14.45 nm, 2.66 nm, and 1.57 nm, respectively. Likewise, the width of the other layers and doping concentration values are presented once again in Fig. 3 so that the reader can follow more easily. The widths of the buffer layer and substrate were not included in the calculations. The attention should be paid that Al doping into the p-doped layer was not considered necessary according to the optimization results as can be seen in Table 1. In this manner, GaN has been specified as the p-layer (see Fig. 3). The next step of the V_{pn} adjustment was taken after getting the best results which includes operating voltage upper limit calculations.

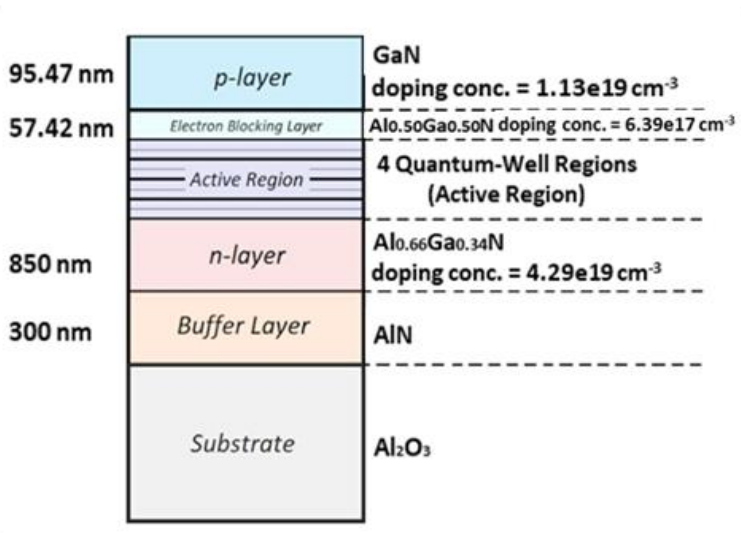

Figure 3. Schematics of the optimized multi QW UV-C AlGaN-based LED.

In Fig. 4(a), the distribution of IQE and input power with respect to V_{pn} is plotted. The LED can operate up to 5.20 V where afterwards a breakdown occurs. Required input power also increases by V_{pn} which fails the success criteria over 5.05 V. Figure 4(b) shows emitted photon wavelength which reaches its peak intensity at 285 nm corresponding to UV-C region.

Efficiency improvement of III-V compound light emission mechanism mostly depends on threading dislocation densities (TDDs), low p-type concentrations, and the light extraction efficiency (LEE) [50]. Among these, the most efficient contribution comes from reduction of the TDD. In other words,

JSR A
Journal of Scientific Reports

growing III-V compunds with a low threading dislocation density still continues to be main issues of experimental studies. In this regard, Hirayama et al. reported the highest relative IQE value of 86% predicted from a relation that assumes a 100% IQE at low temperature [41] and IQE was calculated as 85% by the same approach in a different study [42]. Hao et al. have achieved the value of 77% by reducing TDD [43] and a similar method has also been addressed by Dong et al. via a device based on nano patterned sapphire substrates. Increment on IQE values from 30% to 43% was achieved [44]. The authors of another study have achieved a quite well IQE value of 29% [45].

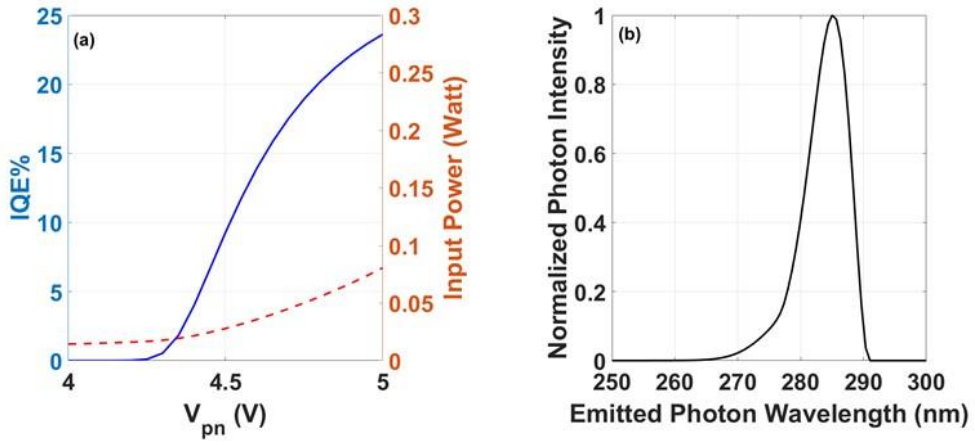

Figure 4. (a) V_{pn} dependence of internal quantum efficiency (solid line) and operating power (dashed line) were given. (b) Emitted light normalized intensity distribution was plotted (peak wavelength at 285 nm.

Besides, GaN based device efficiencies are addressed both theoretically and experimentally by dislocation density effects [51]. These researches clearly show that TDD should be considered to present more realistic results since it directly depends on the growth methods like MBE or MOCVD. TDD is still in improvement process by current experimental technology development studies.

Another effect arises because of nonradiative Auger recombination (c_{Auger}) as mentioned above. However; compounds do not have certain c_{Auger} values in the literature while they are usually accepted within an approximate range. One should note that, these parameters cannot be improved by design optimization. Nevertheless, these uncertainties necessitate an IQE scan of a parameter window constituted by c_{Auger} and c_{recomb} in order to include possible fabrication error and material effects. Therefore, IQE distribution was computed and plotted (see Figure 5) which covers a range of c_{Auger} between 10^{-30} – 10^{-32} cm^6s^{-1}. All other physical parameters are kept nominal as given in Table 1. The figure shows that especially c_{recomb} has a remarkable effect on the internal efficiency.

A final computation was done in order to find the LEE of the structure. The exact design given in Figure 3 was transferred to a finite-difference time-domain software package (MEEP) [52]. The result

JSR A
Journal of Scientific Reports

shows that the deep UV LED design has a LEE value of 34% that leads an overall 8.2% external quantum efficiency (EQE). Huge part of the loss occurs due to non-negligible absorption coefficients of the semiconductor alloys. This situation directly implies a possible improvement by an optimization method on the extraction efficiency which was held out of the scope of this study.

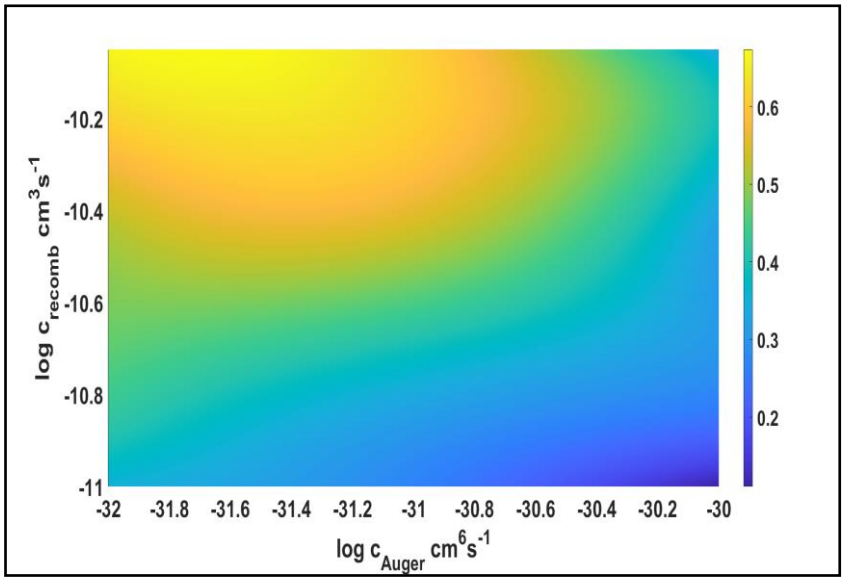

Figure 5. Radiative and nonradiative recombination dependence of IQE.

4. CONCLUSION

This research discusses the IQE improvement of DUV LED design. The analysis technique includes an implementation of a customized genetic algorithm on nanostructure quantum electronic simulations. The widths and doping concentrations of the constituents (EBL, QW, p- and n-doped layers) that gave the best results have been obtained. The main recombination parameters such as c_{Auger}, c_{recomb}, τ_n, and τ_p were taken into consideration in all simulations. Additionally, a parameter window of these recombinations have been presented to show the efficiency dependence. The AlGaN UV-C LED addressed in the current study satisfies the success criteria determined up to 5.05 V according to the V_{pn} dependence of IQE. Standard design with 15 degrees of freedom let the IQE value to be 24% which can be increased over 50% by decreased TDD and up to 70% by an additional reduced Auger recombination. This result is remarkably high considering the output peak wavelength of 285 nm comparable to the prominent studies. Another advantage of the study lies beneath the low operation input power (below 0.1 W/mm^2) requirement at room temperature. Although they are excluded from the scope of this study, LEE and EQE values, which can be further improved by optimization, have also been calculated to get a realistic idea about the device efficiency.

ACKNOWLEDGEMENT

The nanostructure quantum electronic simulation nextnano has been employed in the first optimization step on internal quantum efficiency. We would like to thank Dr. Stefan BIRNER and the team for their understanding and contribution in using the package.

Authors' Contribution
The first author contributed 40% to this study and remaining 60% has been shared as 35% and 25% by the second and third authors, respectively.

REFERENCES

[1] Shur, M., (2021), Emerging applications of deep ultraviolet light emitting diodes, in UV and Higher Energy Photonics: From Materials to Applications 2021 Proceedings, International Society for Optics and Photonics, 11801, 1180105.

[2] Li, J., Gao, N., Cai, D., Lin, W., Huang, K., Li, S., and Kang, J., (2021), Multiple fields manipulation on nitride material structures in ultraviolet light-emitting diodes, Light: Science & Applications, 10, 1-20.

[3] Raeiszadeh, M. and Adeli, B., (2020), A critical review on ultraviolet disinfection systems against COVID-19 outbreak: Applicability, validation, and safety considerations, ACS Photonics, 7, 2941-2951.

[4] Takano, T., Mino, T., Sakai, J., Noguchi, N., Tsubaki, K., and Hirayama, H., (2017), Deep-ultraviolet light-emitting diodes with external quantum efficiency higher than 20% at 275 nm achieved by improving light-extraction efficiency, Applied Physics Express, 10, 031002.

[5] Chang, J.C., Ossoff, S.F., Lobe, D.C., Dorfman, M.H., Dumais, C.M., Qualls, R.G., and Johnson, J.D., (1985), UV inactivation of pathogenic and indicator microorganisms, Applied and environmental microbiology, 49, 1361-1365.

[6] Kowalski, W., (2009), UVGI disinfection theory, in Ultraviolet germicidal irradiation handbook, Springer, Berlin, Heidelberg, 17-50.

[7] Zollner, C.J., DenBaars, S.P., Speck, J., and Nakamura, S., (2021), Germicidal ultraviolet LEDs: a review of applications and semiconductor technologies, Semiconductor Science and Technology, 36, 123001.

[8] SaifAddin, B.K., Almogbel, A.S., Zollner, C.J., Wu, F., Bonef, B., Iza, M., ... and Speck, J.S., (2020), AlGaN deep-ultraviolet light-emitting diodes grown on SiC substrates, ACS Photonics, 7, 554-561.

[9] Lui, G.Y., Roser, D., Corkish, R., Ashbolt, N.J., and Stuetz, R., (2016), Point-of-use water disinfection using ultraviolet and visible light-emitting diodes, Science of the Total Environment, 553, 626-635.

[10] Song, K., Mohseni, M., and Taghipour, F., (2016), Application of ultraviolet light-emitting diodes (UV-LEDs) for water disinfection: A review, Water Research, 94, 341-349.

[11] Kheyrandish, A., Mohseni, M., and Taghipour, F., (2017), Development of a method for the characterization and operation of UV-LED for water treatment, Water Research, 122, 570-579.

[12] Vilhunen, S., Särkkä, H., and Sillanpää, M., (2009), Ultraviolet light-emitting diodes in water disinfection, Environmental Science and Pollution Research, 16, 439-442.

[13] Nakamura, S., (1998), The roles of structural imperfections in InGaN-based blue light-emitting diodes and laser diodes, Science, 281, 956-961.

[14] Kneissl, M., Seong, T.Y., Han, J., and Amano, H., (2019), The emergence and prospects of deep-ultraviolet light-emitting diode technologies, Nature Photonics, 13, 233-244.

[15] Amano, H., Collazo, R., De Santi, C., Einfeldt, S., Funato, M., Glaab, J., ... and Zhang, Y., (2020), The 2020 UV emitter roadmap, Journal of Physics D: Applied Physics, 53, 503001.

[16] Demir, İ., (2018), Growth temperature dependency of high Al content AlGaN epilayers on AlN/Al2O3 templates, Cumhuriyet Science Journal, 39, 728-733.

[17] Park, T.H., Lee, T.H., and Kim, T.G., (2019), Al2O3/AlN/Al-based backside diffuse reflector for high-brightness 370-nm AlGaN ultraviolet light-emitting diodes, Journal of Alloys and Compounds, 776, 1009-1015.

[18] Lim, S.H., Shin, E.J., Lee, H.S., Han, S.K., Le, D.D., and Hong, S.K., (2019), Effects of growth rate and III/V ratio on properties of AlN films grown on c-plane sapphire substrates by plasma-assisted molecular beam epitaxy, Korean Journal of Materials Research, 29, 579-585.

[19] Nagasawa, Y. and Hirano, A., (2018), A review of AlGaN-based deep-ultraviolet light-emitting diodes on sapphire, Applied Sciences, 8, 1264.

[20] Park, K.W. and Yun, Y.H., (2020), Effects of AlN buffer layer on optical properties of epitaxial layer structure deposited on patterned sapphire substrate, Journal of the Korean Crystal Growth and Crystal Technology, 30, 1-6.

[21] Ren, Z., Lu, Y., Yao, H.-H., Sun, H., Liao, C.-H., Dai, J., …, and Li, X., (2019), III-nitride deep UV LED without electron blocking layer, IEEE Photonics Journal, 11, 1-11.

[22] Acharya, J., Venkateshh, S., and Ghosh, K., (2021), Engineering the Active Region to Enhance the IQE by ~8% in AlGaN/GaN based UV-C LED, in 2021 International Conference on

Numerical Simulation of Optoelectronic Devices Proceedings, Institute of Electrical and Electronics Engineers, NUSOD 2021, 69-70.

[23] Gao, N., Chen, J., Feng, X., Lu, S., Lin, W., Li, J., Chen, H., Huang, K., and Kang, J., (2021), Strain engineering of digitally alloyed AlN/GaN nanorods for far-UVC emission as short as 220 nm, Optical Materials Express, 11, 1282-1291.

[24] Peng, Y., Guo, X., Liang, R., Cheng, H., and Chen, M., (2017), Enhanced light extraction from DUV-LEDs by AlN-doped fluoropolymer encapsulation, IEEE Photonics Technology Letters, 29, 1151-1154.

[25] Liu, C., Melanson, B., and Zhang, J., (2020), AlGaN-Delta-GaN quantum well for DUV LEDs, Photonics, 7, 87.

[26] Zhuang, Z., Iida, D., and Ohkawa, K., (2020), Enhanced performance of N-polar AlGaN-based deep-ultraviolet light-emitting diodes, Optics Express, 28, 30423-30431.

[27] Tomson, R., Uhlin, F., and Fridolin, I., (2014), Urea Rebound Assessment Based on UV Absorbance in Spent Dialysate, Asaio Journal, 60, 459-465.

[28] Hirayama, H., Kashima, Y., Matsuura, E., Maeda, N., and Jo, M., (2021), Progress on high-power UVC LEDs by increasing light-extraction efficiency, in Light-Emitting Devices, Materials, and Applications XXV, International Society for Optics and Photonics, 11706, 117060G.

[29] Jain, B., Velpula, R.T., Patel, M., Sadaf, S.Md., and Nguyen, H.P.T., (2021), Improved performance of electron blocking layer free AlGaN deep ultraviolet light-emitting diodes using graded staircase barriers, Micromachines, 12, 334.

[30] Zhang, N., Xu, F.J., Lang, J., Wang, L.B., Wang, J.M., Sun, Y.H., ... and Shen, B., (2021), Improved light extraction efficiency of AlGaN deep-ultraviolet light emitting diodes combining Ag-nanodots/Al reflective electrode with highly transparent p-type layer, Optics Express, 29, 2394-2401.

[31] Itokazu, Y., Kuwaba, S., Jo, M., Kamata, N., and Hirayama, H., (2019), Influence of the nucleation conditions on the quality of AlN layers with high-temperature annealing and regrowth processes, Japanese Journal of Applied Physics, 58, SC1056.

[32] Shin, W., Pandey, A., Liu, X., Sun, Y., and Mi, Z., (2019), Photonic crystal tunnel junction deep ultraviolet light emitting diodes with enhanced light extraction efficiency, Optics Express, 27, 38413-38420.

[33] Moe, C.G., Sugiyama, S., Kasai, J., Grandusky, J.R., and Schowalter, L.J., (2018), AlGaN Light- Emitting Diodes on AlN Substrates Emitting at 230 nm, Physica Status Solidi (a), 215, 1700660.

[34] Chen, X. and Wu, Y.R., (2015), Numerical study of current spreading and light extraction in deep UV light-emitting diode, in Light-Emitting Diodes: Materials, Devices, and Applications for Solid State Lighting XIX, International Society for Optics and Photonics, 9383, 93830Q.

[35] Bhattacharyya, A., Moustakas, T.D., Zhou, L., Smith, D.J., and Hug, W., (2009), Deep ultraviolet emitting AlGaN quantum wells with high internal quantum efficiency, Applied Physics Letters, 94, 181907.

[36] Rudinsky, M.E. and Karpov, S.Y., (2020), Radiative and Auger recombination constants and internal quantum efficiency of (0001) AlGaN deep- UV light- emitting diode structures, Physica Status Solidi (a), 217, 1900878.

[37] Bryan, Z., Bryan, I., Xie, J., Mita, S., Sitar, Z., and Collazo, R., (2015), High internal quantum efficiency in AlGaN multiple quantum wells grown on bulk AlN substrates, Applied Physics Letters, 106, 142107.

[38] Lobo-Ploch, N., Mehnke, F., Sulmoni, L., Cho, H.K., Guttmann, M., Glaab, J., … and Kneissl, M., (2020), Milliwatt power 233 nm AlGaN-based deep UV-LEDs on sapphire substrates, Applied Physics Letters, 117, 111102.

[39] Murotani, H., Tanabe, R., Hisanaga, K., Hamada, A., Beppu, K., Maeda, N., ... and Yamada, Y., (2020), High internal quantum efficiency and optically pumped stimulated emission in AlGaN-based UV-C multiple quantum wells, Applied Physics Letters, 117, 162106.

[40] Shim, J.I., Han, D.P., Oh, C.H., Jung, H., and Shin, D.S., (2018), Measuring the internal quantum efficiency of light-emitting diodes at an arbitrary temperature, IEEE Journal of Quantum Electronics, 54, 1-6.

[41] Hirayama, H., Fujikawa, S., Noguchi, N., Norimatsu, J., Takano, T., Tsubaki, K., and Kamata, N., (2009), 222–282 nm AlGaN and InAlGaN- based deep- UV LEDs fabricated on high-quality AlN on sapphire, Physica Status Solidi (a), 206, 1176-1182.

[42] Wang, T.Y., Tasi, C.T., Lin, C.F., and Wuu, D.S., (2017), 85% internal quantum efficiency of 280-nm AlGaN multiple quantum wells by defect engineering, Scientific Reports, 7, 1-8.

[43] Hao, G.D., Tamari, N., Obata, T., Kinoshita, T., and Inoue, S.I., (2017), Electrical determination of current injection and internal quantum efficiencies in AlGaN-based deep-ultraviolet light-emitting diodes, Optics Express, 25, A639-A648.

[44] Dong, P., Yan, J., Zhang, Y., Wang, J., Zeng, J., Geng, C., ... and Li, J., (2014), AlGaN-based deep ultraviolet light-emitting diodes grown on nano-patterned sapphire substrates with significant improvement in internal quantum efficiency, Journal of Crystal Growth, 395, 9-13.

[45] Guttmann, M., Susilo, A., Sulmoni, L., Susilo, N., Ziffer, E., Wernicke, T., and Kneissl, M., (2021), Light extraction efficiency and internal quantum efficiency of fully UVC-transparent AlGaN based LEDs, Journal of Physics D: Applied Physics, 54, 335101.

[46] Trellakis, A., Zibold, T., Andlauer, T., Birner, S., Smith, R.K., Morschl, R., and Vogl, P., (2006), The 3D nanometer device project nextnano: Concepts, methods, results, Journal of Computational Electronics, 5, 285–289.

[47] Birner, S., Zibold, T., Andlauer, T., Kubis, T., Sabathil, M., Trellakis, A., and Vogl, P., (2007), Nextnano: general purpose 3-D simulations, IEEE Transactions on Electron Devices, 54, 2137-2142.

[48] Dmitriev, A. and Oruzheinikov, A., (1999), The rate of radiative recombination in the nitride semiconductors and alloys, Journal of Applied Physics, 86, 3241-3246.

[49] Nippert, F., Tollabi Mazraehno, M., Davies, M.J., Hoffmann, M.P., Lugauer, H.J., Kure, T., ... and Wagner, M.R., (2018), Auger recombination in AlGaN quantum wells for UV light-emitting diodes, Applied Physics Letters, 113, 071107.

[50] Hirayama, H., Fujikawa, S., and Kamata, N., (2015), Recent progress in AlGaN- based deep-UV LEDs, Electronics and Communications in Japan, 98, 1-8.

[51] Yu, J., Hao, Z., Li, L., Wang, L., Luo, Y., Wang, J., and Li, H., (2017), Influence of dislocation density on internal quantum efficiency of GaN-based semiconductors, AIP Advances, 7, 035321.

[52] A. F. Oskooi, D. Roundy, M. Ibanescu, P. Ber-mel, J. D. Joannopoulos, and S. G. Johnson (2010), Meep: A flexible free-software package for electromagnetic simulations by the FDTD method, Computer Physics Communications, 181, 687-702.